

Relationship of chlorophyll to phosphorus and nitrogen in nutrient-rich lakes

Christopher T. Filstrup & John A. Downing

To cite this article: Christopher T. Filstrup & John A. Downing (2017) Relationship of chlorophyll to phosphorus and nitrogen in nutrient-rich lakes, *Inland Waters*, 7:4, 385-400, DOI: [10.1080/20442041.2017.1375176](https://doi.org/10.1080/20442041.2017.1375176)

To link to this article: <https://doi.org/10.1080/20442041.2017.1375176>



© 2017 The Author(s). Published by Informa UK Limited, trading as Taylor & Francis Group



[View supplementary material](#)



Published online: 09 Oct 2017.



[Submit your article to this journal](#)



Article views: 6722



[View Crossmark data](#)

Relationship of chlorophyll to phosphorus and nitrogen in nutrient-rich lakes

Christopher T. Filstrup,  and John A. Downing 

Large Lakes Observatory and Minnesota Sea Grant, University of Minnesota Duluth, Duluth, USA

ABSTRACT

Nitrogen (N) and phosphorus (P) commonly co-limit primary productivity in lakes, and chlorophyll *a* (Chl-*a*) is predicted to be greatest under high N, high P regimes. Because land use practices can alter N and P biogeochemical cycles in watersheds, it is unclear whether previously documented phytoplankton–nutrient relationships apply where landscapes are highly disturbed. Here, we analyzed a lake water quality database from an agricultural region to explore relationships among Chl-*a*, total N (TN), and total P (TP) under extreme nutrient concentrations. Chl-*a* was weakly related to TN when TP was $\leq 100 \mu\text{g L}^{-1}$ but displayed a stronger response to TN at higher TP. When TP exceeded $100 \mu\text{g L}^{-1}$, Chl-*a* increased with increasing TN until reaching a TN threshold of $\sim 3 \text{ mg L}^{-1}$ and decreased thereafter, resulting in a high nutrient, low Chl-*a* region that did not coincide with shifts in nutrient limitation, light availability, cellular Chl-*a* content, phytoplankton composition, or zooplankton grazing pressure. Beyond the threshold, nitrate comprised most of TN and occurred with reduced dissolved organic matter (DOM). These observations suggest that photolysis of nitrate may produce reactive oxygen species that damage DOM and phytoplankton. Reduction in N loading at high P could therefore increase Chl-*a* and decrease water clarity, resulting in an apparent worsening of water quality. Our data suggest that monitoring Chl-*a* or Secchi depth may fail to indicate water quality degradation by extreme nutrient concentrations. These findings highlight how extreme nutrient regimes in lakes can produce novel relationships between phytoplankton and nutrients.

KEYWORDS

chlorophyll *a*; eutrophication; lakes; nitrate; nitrogen; phosphorus


Introduction

Current debate regarding nutrient management strategies to mitigate cultural eutrophication in lakes (e.g., Schindler et al. 2008, Scott and McCarthy 2010, Paerl et al. 2016, Schindler et al. 2016) warrants further study of phytoplankton–nutrient relationships. Early empirical studies of these relationships focused largely on phosphorus (P) because it was demonstrated to limit primary productivity in most lakes (Vollenweider 1968, Edmondson 1970, Schindler 1977). In temperate lakes, chlorophyll *a* (Chl-*a*) could be predicted as a positive log-linear function of total P (TP; Sakamoto 1966, Dillon and Rigler 1974, Jones and Bachmann 1976), thereby supporting P-limitation of primary productivity in lakes. Although log-linear models nicely predicted Chl-*a* from TP in some lakes or regions, they tended to over-predict Chl-*a* at high TP across large TP gradients using global datasets, resulting in Chl-*a*–TP relationships better described as sigmoidal functions on log-transformed scales (McCauley et al. 1989). Although Chl-*a* response to TP in individual lakes may differ from global empirical models (Smith and

Shapiro 1981), the upper Chl-*a* threshold to increasing TP suggested that another resource, such as nitrogen (N) or light, becomes limiting under high TP. While early whole ecosystem nutrient manipulations focused on oligotrophic lakes, where P-limitation was likely, phytoplankton biomass may commonly be limited by multiple nutrients in more productive lakes, especially over shorter temporal scales (see Sterner 2008).

The influences of N or N:P ratios on phytoplankton biomass are well established, and current evidence strongly supports N and P co-limitation of primary productivity in most lakes and synergistic responses of phytoplankton to dual (N+P) nutrient enrichment (Elser et al. 2007, Allgeier et al. 2011, Bracken et al. 2015). In addition to Chl-*a*–TP relationships, Sakamoto (1966) observed a strong log-linear relationship between Chl-*a* and total N (TN) in Japanese lakes, where deviations from these relationships were hypothesized to result from changing nutrient supply ratios (i.e., N:P). Subsequent studies found that either TN or TN:TP ratios, in addition to TP,

CONTACT Christopher T. Filstrup  filstrup@d.umn.edu

 Supplemental data for this article can be accessed [here](#).

improved predictive relationships for Chl-*a* across large N:P gradients (Smith 1982, Canfield 1983). TN:TP ratios can influence parameter estimates (i.e., slope and intercept) of log-linear relationships between Chl-*a* and either TN or TP, despite Chl-*a* being well correlated to individual nutrients across the entire TN:TP gradient (Prairie et al. 1989). Within a classification and regression tree framework, TN:TP ratios were often selected as an important factor in classifying lakes to improve Chl-*a* predictions from TP (e.g., Yuan and Pollard 2014). In regions where N-limitation occurs, Chl-*a* may show smaller responses to TP changes, however, and models including TN only may better predict Chl-*a* where N-limitation is common (Smith and Shapiro 1981, Jones et al. 1989).

N and P cycles can be coupled in lakes and streams (Finlay et al. 2013, Gibson et al. 2015), but human activities within watersheds may alter natural biogeochemical cycles. Agricultural practices such as fertilizer amendments or manure application not only contribute to increased N loads in receiving streams but can also cause shifts in the dissolved N pool (Howarth et al. 1996, Stanley and Maxted 2008). Eutrophic lakes can have low TN:TP compared to lakes in watersheds with natural land cover, although ratios depend on the type of agriculture (Downing and McCauley 1992). While lakes in regions with large-scale animal agriculture can have low TN:TP, lakes in regions dominated by row-crops commonly have high TN:TP (Arbuckle and Downing 2001). For example, high TN:TP loads from receiving streams in agricultural regions can maintain strict P-limitation of primary productivity (Vanni et al. 2011), whereas systems may be driven to N-limitation in livestock production regions. Additionally, watershed permeability and climate interact with land use and land cover to modify the effect of agricultural practices on lake nutrients (Fraterrigo and Downing 2008, Hayes et al. 2015). Because agricultural practices may modify N and P biogeochemical cycles, empirical relationships between phytoplankton and nutrients developed from regions with more diverse landscape characteristics may not apply to intense agricultural regions.

Previous studies have demonstrated that regional landscape characteristics can modify Chl-*a*-TP relationships in lakes. For example, Jones et al. (2011) showed that the maximum Chl-*a* concentration observed for a given TP differed among lake datasets spanning different geographic extents. When modeled as log-linear relationships, the slopes of Chl-*a*-TP relationships for individual regions within the United States were positively related to proportion of pasturelands, whereas the intercepts of these models were negatively related to proportion of wetlands, which are often negatively correlated to agricultural land use (Wagner et al. 2011). By using the same dataset to model relationships using sigmoidal functions, Filstrup

et al. (2014b) demonstrated that regional maximum Chl-*a* observed under high TP conditions was greater in regions with more pasturelands, whereas Chl-*a*-TP relationships were steeper in regions with less wetland cover. Although these studies showed that agricultural practices could modify Chl-*a* response to TP gradients, they did not consider the role of N in shaping these relationships.

In this study, we analyzed a 13-year water quality database for 139 lakes located within an intense agricultural region to examine phytoplankton biomass-nutrient relationships in mesotrophic to hypereutrophic lakes. Specifically, we were interested in how Chl-*a* would respond to nearly orthogonal gradients in TN and TP in these lakes and whether or not empirical relationships among Chl-*a*, TN, and TP developed from other regions would hold in this disturbed region with extreme nutrient concentrations. Based on our findings, we evaluated several potential mechanisms, including shifts in nutrient limitation, light availability, cellular Chl-*a* content, phytoplankton composition, zooplankton grazing pressure, and nitrate-derived reactive oxygen species (ROS) to help explain relationships observed in this region.

Methods

Study region

To test our hypotheses, we analyzed a water quality dataset from an intensively managed agricultural region in the Midwestern United States. Agriculture accounts for ~90% of land use and land cover in this region, with coverage relatively consistent since the early 1900s (Arbuckle and Downing 2001, Heathcote and Downing 2012). The Iowa Lake Monitoring Program dataset contains physical, chemical, and plankton compositional data from 139 lakes located within the state of Iowa (Fig. 1). Most of the lakes in the dataset are manmade ($n = 107$), including 4 large reservoirs and 10 surface mine lakes. Of the 32 natural lakes, 7 were oxbows and 1 was a shallow, emergent macrophyte-dominated lake. Because of these diverse origins, lakes varied widely in surface area (0.04–60.39 km²), maximum depth (1.2–39.6 m), and watershed to lake area ratio (0.3–763.6). These lakes are classified as mesotrophic to hypereutrophic and receive high external nutrient loading rates from their watersheds that support large phytoplankton biomasses (Jones et al. 1976, Stenback et al. 2011), commonly dominated by Cyanobacteria (Filstrup et al. 2016).

Sample collection and field observations

Lakes were sampled at their historically deepest point 3 times per year from 2001 to 2014, when possible, excluding

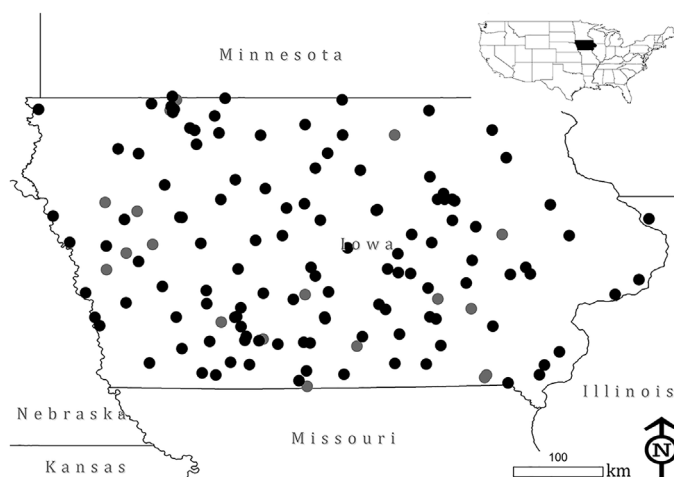


Figure 1. Study area indicating location of lakes, all lakes located within the state boundaries of Iowa, although some crossed into bordering states. Black points indicate lakes with observed total phosphorus $>100 \mu\text{g L}^{-1}$; gray points indicate lakes with observed total phosphorus $\leq 100 \mu\text{g L}^{-1}$.

a program hiatus in 2008. Multiple sampling events per lake were intended to characterize water quality conditions in early (mid-May–Jun; Round 1), mid (Jul–mid-Aug; Round 2), and late summer (mid-Aug–Sep; Round 3). Nutrient and phytoplankton samples were collected as surface mixed-layer samples using either flexible tubing and a pump (prior to 2006) or an integrated water column sampler to the depth of the thermocline (maximum depth of 2.0 m beginning in 2006). Zooplankton samples were collected using a Wisconsin net (63 μm mesh) by vertically towing the net from the thermocline to the lake surface. Phytoplankton and zooplankton samples were preserved in the field with Lugol's solution (APHA 1998) and formalin (Haney and Hall 1973), respectively. All samples were stored on ice in the field, and chemical samples were stored at 4 °C on return to the laboratory.

Water transparency and mixing depth were recorded in the field and used to estimate underwater light climate experienced by phytoplankton. Water transparency was measured as Secchi depth (z_{Secchi}). Mixing depth (z_{mix}) was determined from vertical temperature profiles recorded using a multiparameter data sonde. Thermocline depth was identified as the depth of the maximal rate of change in temperature, where temperature change was $>1 \text{ }^\circ\text{C m}^{-1}$ (Kalff 2001). The Secchi depth to mixing depth ratio ($z_{\text{Secchi}}:z_{\text{mix}}$) was calculated as an estimate of the proportion of time phytoplankters remain in the euphotic zone.

Laboratory analyses

Chl-*a*, TP, TN, nitrate + nitrite (hereafter nitrate), ammonium + ammonia (hereafter ammonium), and dissolved organic carbon (DOC) were analyzed within 36 h of sampling or preserved for later analyses. Chl-*a* samples were

filtered (GF/C filter), extracted in 100% acetone, and analyzed using the nonacidified fluorometry method (Arar and Collins 1997, Wright et al. 1997). TP samples were digested with persulfate and analyzed using the ascorbic acid method (APHA 1998). TN samples were digested with persulfate and analyzed using the second-derivative spectroscopy method (Crompton et al. 1992). To investigate dissolved inorganic N (DIN) composition, we analyzed nitrate and ammonium samples using the second-derivative ultraviolet spectroscopy method (Crompton et al. 1992) and either manual or semiautomated phenate methods on filtered (0.45 μm) water samples (USEPA 1993, APHA 1998), respectively. DOC samples were filtered (0.45 μm), acidified, and analyzed using the high-temperature combustion method (APHA 1998).

Phytoplankton and zooplankton samples were analyzed using light microscopy to calculate taxonomic biovolume and biomass, respectively, as described by Filstrup et al. (2014a). Phytoplankters were identified to genus, counted and measured (first 50 individuals per genera) using an inverted microscope (Lund et al. 1958, APHA 1998), and quantified as biovolume using taxon-specific linear measures (Hillebrand et al. 1999). Zooplankters were identified to genus for cladocerans and for copepods, counted and measured using a stereoscopic microscope (APHA 1998), and quantified as biomass using published length–biomass relationships (Dumont et al. 1975, McCauley 1984).

Statistical considerations

Although previous studies of phytoplankton–nutrient relationships primarily analysed data using seasonal averages, data were analysed here as individual sampling events to allow analyses across the widest range in nutrients.

Although this approach introduces issues with sample independence (i.e., multiple observations per year per lake), the high degree of landscape modification within this region contributes to lakes that change rapidly in nutrient and phytoplankton conditions. To visualize phytoplankton biomass response to TN and TP, we created contour plots of Chl-*a* and total phytoplankton biomass with local polynomial smoothing (second-degree polynomial) to grid data using Surfer 8 software (Golden Software, LLC; Golden, CO, USA). All data were retained in the analyses (i.e., no filtering), and contours were not extrapolated beyond the range of data. This approach was also used to visualize underwater light conditions ($z_{\text{Secchi}}:z_{\text{mix}}$ contours) across lake nutrient space. All other analyses were performed using the program R (R Core Team 2016). Ordinary least squares regression was used to model Chl-*a* as a function of (1) TP only; (2) TN and TP; and (3) TN, TP, and $z_{\text{Secchi}}:z_{\text{mix}}$, where linear, squared, and cubed predictors and a TN \times TP interaction term were included in models. We did not include interaction terms between TN or TP and $z_{\text{Secchi}}:z_{\text{mix}}$ because we could think of no *a priori* theoretical reason to do so. Prior to analyses, predictor variables were visually assessed for multicollinearity. Stepwise selection was used to eliminate or retain predictor variables based on the Akaike Information Criterion (AIC). The 3 competing models were compared using AIC. Because of wide variation among observations, variability in response variables across TN gradients were visualized using boxplots by TN interval (bin width = 0.1 log TN) within *ggplot2* (Wickham 2009). Piecewise linear models of Chl-*a*-N relationships were fit using the package *SiZer* (Sonderegger 2012). LOWESS (locally weighted scatterplot smoothing) lines, in which the smoothing factor (*f*) was set at two-thirds *a priori*, were added to scatterplots to aid with visual interpretation of relationships as needed. Response and predictor variables were \log_{10} -transformed prior to analyses to improve normality and reduce heteroscedasticity, as needed.

Results

Dataset description

Phytoplankton biomass, nutrients, and underwater light climate varied across several orders of magnitude, with observations representing oligotrophic to hypereutrophic conditions included in the dataset (Table 1). Only 0.5% of observations ($n = 24$ of 4561) had TP < 10 $\mu\text{g L}^{-1}$, however. Because of large ranges in TN and TP, TN:TP ratios varied widely, with a median TN:TP of 46.7 by atoms. Water transparency (z_{Secchi}) ranged across 2 orders of magnitude, with 25% of observations having values < 0.5 m. Similarly, $z_{\text{Secchi}}:z_{\text{mix}}$ values suggested that light availability in the surface mixed layer varied from being restricted to the lake

Table 1. Summary statistics for observations of water column chlorophyll *a* (Chl-*a*; $\mu\text{g L}^{-1}$), total phytoplankton biomass (Biomass_{phyto}; mg L^{-1}), total nitrogen (TN; mg L^{-1}), total phosphorus (TP; $\mu\text{g L}^{-1}$), total nitrogen to total phosphorus ratio (TN:TP; by atoms), water transparency (z_{Secchi} ; m), and the Secchi depth to mixing depth ratio ($z_{\text{Secchi}}:z_{\text{mix}}$).

Variable	Average	Median	Minimum	Maximum
Chl- <i>a</i>	40.3	26.0	0.4	743.0
Biomass _{phyto}	130.2	30.2	<0.1	21502.8
TN	2.54	1.56	0.29	23.04
TP	104.6	75.0	5.0	918.5
TN:TP	90.1	46.7	1.5	2023.5
z_{Secchi}	1.2	0.8	0.1	9.5
$z_{\text{Secchi}}:z_{\text{mix}}$	0.35	0.25	0.01	1.00

surface to extending throughout the entire surface mixed layer. Only a quarter of observations had $z_{\text{Secchi}}:z_{\text{mix}} \geq 0.5$, suggesting that phytoplankters spent over half their time in the aphotic zone for most observations.

Empirical relationships among phytoplankton biomass, TN, and TP

Visually, phytoplankton biomass varied across both TN and TP gradients, although relationships between phytoplankton biomass and TN differed depending on TP. For oligotrophic to eutrophic observations (TP $\leq 100 \mu\text{g L}^{-1}$ or 2.0 log units), both Chl-*a* and total phytoplankton biomass were unrelated to TN, as shown by the nearly vertical contour lines (Fig. 2). Chl-*a* and total phytoplankton biomass increased with increasing TP for these observations but did not vary with respect to TN. The region of high total phytoplankton biomass under low TP and high TN (i.e., upper left corner) likely resulted from low sample size ($n = 4$), where 2 observations had total phytoplankton biomass exceeding 100 mg L^{-1} . By contrast, phytoplankton biomass varied with TN for hypereutrophic observations (TP > 100 $\mu\text{g L}^{-1}$ or 2.0 log units). Chl-*a* and total phytoplankton biomass increased with increasing TN and TP, but both were greatest at medium TN (~ 1.6 – 4.0 mg L^{-1} ; 0.2–0.6 log units) and decreased at higher TN for these observations. The high nutrient, low Chl-*a* region (HNLC; i.e., upper right corner) contained 271 observations from 64 different lakes spanning the entire study period. Median Chl-*a* was 20 $\mu\text{g L}^{-1}$ (interquartile range [IQR]: 7–46 $\mu\text{g L}^{-1}$) for this region compared to 62 $\mu\text{g L}^{-1}$ (IQR: 31–107 $\mu\text{g L}^{-1}$) for the Chl-*a* maximum region. In the bottom right corner were 3 observations with Chl-*a* exceeding 200 $\mu\text{g L}^{-1}$, which likely inflated Chl-*a* contour values in this low sample size region ($n = 47$).

Ordinary least squares regression further supported both TN and TP as significant predictors of Chl-*a* across all observations, although the best model also included $z_{\text{Secchi}}:z_{\text{mix}}$ (Table 2). The TP-only model ($F_{2,4558} = 927.1$; $p < 0.001$) explained 29% of the variance in \log_{10} Chl-*a* and

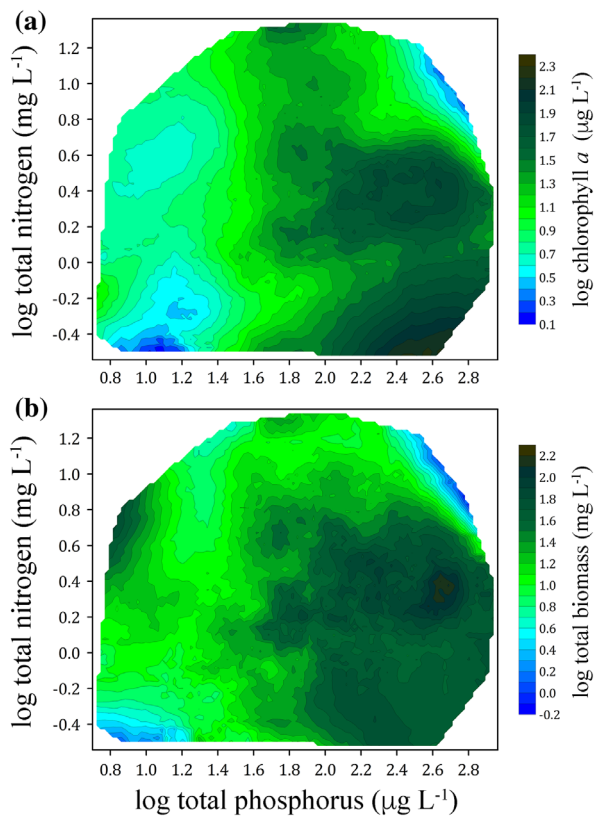


Figure 2. (a) Chlorophyll *a* and (b) total phytoplankton biomass contour plots on total nitrogen vs. total phosphorus nutrient space. Contour lines were generated using second-degree local polynomial regression of lake observational data. All variables were \log_{10} -transformed prior to analyses.

included significant squared and cubed TP terms. The TN and TP model ($F_{6,4554} = 371.0$; $p < 0.001$) explained slightly more variance in \log_{10} Chl-*a* (adj. $r^2 = 0.33$) and included significant linear and nonlinear terms for TN and TP, as well as a significant TN \times TP interaction term. The TN and TP model ($AIC_{TN+TP} = 5177.9$) was selected as the better fitting model compared to the TP-only model ($AIC_{TP} = 5428.4$) despite the slight improvement in explained variance. A third model including significant linear and nonlinear terms for TN, TP, and $z_{\text{Secchi}}:z_{\text{mix}}$ ($F_{9,4551} = 323.4$; $p < 0.001$) was selected as the best Chl-*a* predictive model overall ($AIC_{TN+TP+LIGHT} = 4744.0$) by explaining 39% of the variance in \log_{10} Chl-*a*. Although linear terms of model predictors were significantly correlated ($\alpha = 0.05$), correlations were weak, with the strongest correlation occurring between TP and $z_{\text{Secchi}}:z_{\text{mix}}$ ($r = -0.48$; Supplemental Fig. S1).

Despite considerable overlap, Chl-*a* distributions for individual TN intervals further suggested differences in Chl-*a*-TN relationships for different trophic conditions (Fig. 3). For oligotrophic combined with mesotrophic ($TP < 30 \mu\text{g L}^{-1}$ or 1.48 log units) and eutrophic ($30 \mu\text{g L}^{-1} \leq TP \leq 100 \mu\text{g L}^{-1}$) conditions, Chl-*a* distributions increased with increasing

TN but were relatively consistent beyond a TN of ~ 1.6 and 2.0 mg L^{-1} (0.2 and 0.3 log units), respectively, thereby resembling a positive asymptotic relationship (Fig. 3a and b). Because sample size was low, trends in Chl-*a* distributions across TN gradients were not as smooth for oligotrophic plus mesotrophic observations ($n = 580$) compared to eutrophic observations ($n = 2370$). For hypereutrophic observations ($TP > 100 \mu\text{g L}^{-1}$), however, Chl-*a* distributions across the TN gradient approximated a unimodal (“hump-shaped”) response curve when excluding several high Chl-*a* distributions at low TN (Fig. 3c). Median Chl-*a* decreased rapidly with increasing TN after reaching a maximum concentration and remained at consistently low concentrations for the highest TN intervals.

When modeled, the relationship between Chl-*a* and TN for hypereutrophic observations was better approximated by a piecewise linear model rather than a linear model (Fig. 4). Although the linear regression model was significant ($F_{1,1609} = 77.8$; $p < 0.001$), TN explained little variance in Chl-*a* (adj. $r^2 = 0.05$) across the entire TN range. The linear regression over-predicted Chl-*a* at TN extremes and under-predicted them at medium TN. The piecewise linear model revealed a significant negative relationship between Chl-*a* and TN ($F_{1,401} = 68.7$; $p < 0.001$)

Table 2. Least squares regression models of chlorophyll *a* ($\mu\text{g L}^{-1}$; \log_{10} -transformed) predicted by total phosphorus (TP)-only ($\mu\text{g L}^{-1}$; \log_{10} -transformed); TP and total nitrogen (TN; mg L^{-1} ; \log_{10} -transformed); and TP, TN, and Secchi depth to mixing depth ratio ($z_{\text{Secchi}}:z_{\text{mix}}$). Linear, squared, and cubed terms of predictor variables as well as an interaction term between TN and TP were considered. Predictor variables were entered or removed using stepwise selection and retained based on Akaike Information Criterion (AIC). Significance was evaluated at $\alpha = 0.05$. SE = standard error; NS = not significant.

Parameter	Estimate	SE	<i>t</i> -value	<i>p</i> -value
Model 1. TP only: $F_{2,4558} = 927.1$; $p < 0.001$; adj. $r^2 = 0.29$				
Intercept	-0.259	0.053	-4.919	<0.001
(log TP) ²	0.956	0.042	22.931	<0.001
(log TP) ³	-0.258	0.014	-18.523	<0.001
Model 2. TP + TN: $F_{6,4554} = 371.0$; $p < 0.001$; adj. $r^2 = 0.33$				
Intercept	1.408	0.433	3.253	<0.001
log TP	-2.468	0.720	-3.428	<0.001
(log TP) ²	2.100	0.390	5.392	<0.001
(log TP) ³	-0.420	0.068	-6.136	<0.001
log TN	1.500	0.109	13.713	<0.001
(log TN) ²	-0.486	0.050	-9.734	<0.001
log TP \times log TN	-0.625	0.061	-10.335	<0.001
Model 3. TP + TN + $z_{\text{Secchi}}:z_{\text{mix}}$: $F_{9,4551} = 323.4$; $p < 0.001$; adj. $r^2 = 0.39$				
Intercept	1.792	0.414	4.333	<0.001
log TP	-2.432	0.689	-3.530	<0.001
(log TP) ²	1.823	0.373	4.884	<0.001
(log TP) ³	-0.342	0.066	-5.212	<0.001
log TN	1.426	0.105	13.637	<0.001
(log TN) ²	-0.350	0.048	-7.249	<0.001
$z_{\text{Secchi}}:z_{\text{mix}}$	1.051	0.235	4.470	<0.001
$(z_{\text{Secchi}}:z_{\text{mix}})^2$	-3.211	0.545	-5.894	<0.001
$(z_{\text{Secchi}}:z_{\text{mix}})^3$	1.798	0.350	5.134	<0.001
log TP \times log TN	-0.638	0.058	-11.015	<0.001

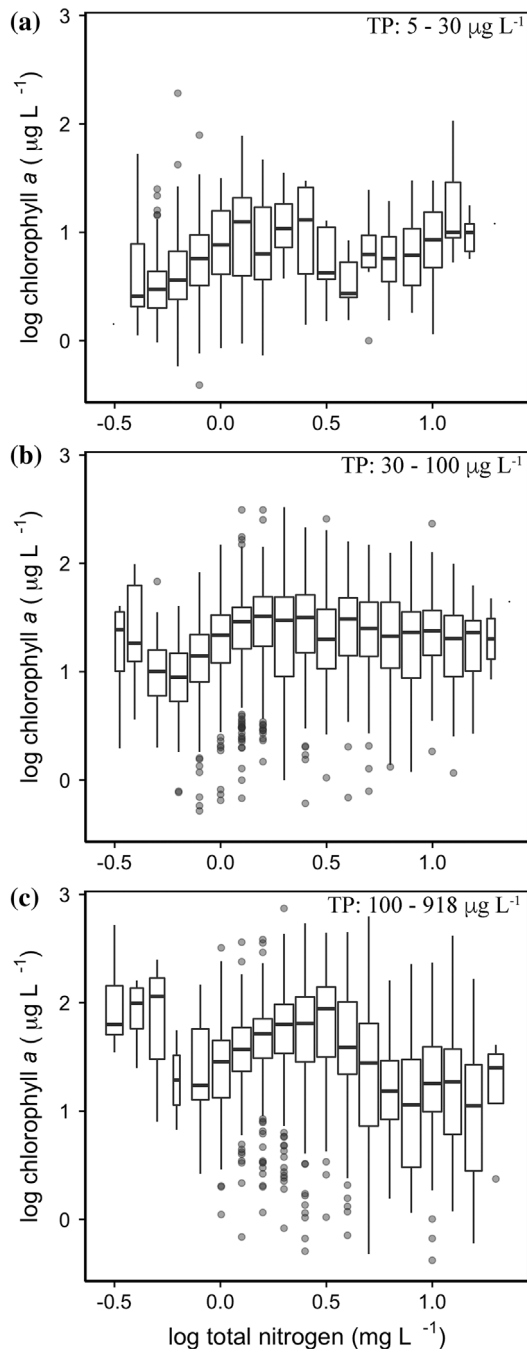


Figure 3. Boxplots of chlorophyll *a* concentrations by total nitrogen interval (bin width = 0.1 log total nitrogen) for (a) oligotrophic and mesotrophic, (b) eutrophic, and (c) hypereutrophic observations. Total phosphorus (TP) ranges of observations are provided for each panel. Markers representing outliers are transparent, so darker clusters represent overlapping markers. All variables were \log_{10} -transformed prior to analyses.

for $\text{TN} > 2.93 \text{ mg L}^{-1}$ (0.47 log units) that explained 14% of Chl-*a* variance. Below this threshold, Chl-*a* and TN were unrelated ($F_{1, 1206} = 18.0$; $p < 0.001$; adj. $r^2 = 0.01$). Confidence intervals (CI: 97.5%) for the threshold estimate were $2.26\text{--}3.24 \text{ mg L}^{-1}$ (0.35–0.51 log units).

Hypotheses to explain the high nutrient, low Chl-*a* region

Because finding a region of HNLC at extreme TN concentrations requires explanation, we tested 4 potential interpretations for this pattern. They posit that the HNLC region coincided with (1) shifts in resource limitation due to nutrient and light deficiency, (2) phytoplankton phenology or reduced cellular Chl-*a* content, (3) high zooplankton grazing pressure, or (4) increased damage to phytoplankton under high N concentrations.

Resource limitation hypothesis

We tested whether the HNLC region coincided with shifts in nutrient deficiency. For hypereutrophic observations, TN:TP varied from 2 to 385 (by atoms), suggesting that both N- and P-deficient growth conditions were represented in the dataset, but the pattern in these values across the Chl-*a*–TN relationship did not support this hypothesis. Growth conditions were mostly P-deficient above the TN threshold (2.9 mg L^{-1} or ~ 0.5 log units) but were a mixture of balanced and N-deficient conditions below the threshold, with the latter predominating at the lowest TN (Fig. 5). Because growth conditions were inferred from TN:TP ratios based on previous empirical analyses (Guildford and Hecky 2000), we also evaluated changes in nitrate and soluble reactive phosphorus (SRP) concentrations across the Chl-*a*–TN relationship. As anticipated, nitrate concentrations in the water column were relatively low when TN:TP was < 20 by atoms (i.e., N deficiency) and relatively high when TN:TP was > 50 by atoms (i.e., P deficiency; Fig. 5a). SRP concentrations were more variable relative to growth status, but the highest concentrations most commonly occurred under N deficiency, whereas smaller concentrations were found under P-deficient and balanced growth conditions (Fig. 5b). If Chl-*a* was primarily responding to a shift toward P deficiency above the TN threshold, then Chl-*a* concentrations would be unrelated to TN (i.e., flat relationship) rather than displaying a significant decrease (Fig. 4).

Because $z_{\text{Secchi}}:z_{\text{mix}}$ was a significant predictor of Chl-*a* (Table 2), we tested whether the HNLC region coincided with reduced light availability in the surface mixed layer. Contours of $z_{\text{Secchi}}:z_{\text{mix}}$ plotted on TN and TP space largely mirrored Chl-*a* contours, in which low $z_{\text{Secchi}}:z_{\text{mix}}$ coincided with high Chl-*a* and vice versa (c.f. Fig. 6 and 2a). As an exception, some of the lowest $z_{\text{Secchi}}:z_{\text{mix}}$ contours occurred in the HNLC region, suggesting that these low values did not solely result from Chl-*a* concentrations. Distributions of $z_{\text{Secchi}}:z_{\text{mix}}$ were not significantly lower for the highest TN intervals, however, and actually displayed a trend toward increasing $z_{\text{Secchi}}:z_{\text{mix}}$ (Fig. 7).

Phytoplankton composition hypothesis

We tested whether phytoplankton phenology or shifts in cellular Chl-*a* content of dominant taxa aligned with the Chl-*a*–TN pattern for hypereutrophic observations. Because each lake was sampled 3 times from mid-May through September, the timing of TN pulses from the watershed (e.g., early summer storm events) may have yielded high TN before phytoplankton biomass had time to develop, but these pulses could also have diluted existing lake phytoplankton biomass with storm runoff or coincided with large loads of inorganic particles that reduce light availability. Observations from mid-summer (Round 2) and early autumn (Round 3) composed the majority of observations at medium TN (Fig. 8a). Above the TN threshold, however, observations shifted to predominantly from early summer (Round 1). TN and surface water temperature were significantly but weakly correlated ($r = -0.26$; $p < 0.001$), however, suggesting that TN was also responding to other factors besides season. We also examined whether the HNLC region coincided with reduced cellular Chl-*a* content (Chl-*a*:biomass ratio). Chl-*a*:biomass ratios were relatively constant for individual TN intervals across the entire range of TN for hypereutrophic observations (Fig. 8b). Additionally, Cyanobacteria consistently composed the majority of phytoplankton biomass below the TN threshold and generally decreased with increasing TN above the threshold (Supplemental Fig. S2), which counters the hypothesis that the HNLC region coincided with a shift toward Cyanobacteria dominance. These findings support prior analyses in which contour plots displayed consistent patterns for Chl-*a* and phytoplankton biomass (Fig. 2).

Zooplankton grazing hypothesis

We tested if the HNLC region coincided with high crustacean zooplankton biomass, which may have influenced Chl-*a* through top-down mechanisms that could have uncoupled Chl-*a*–nutrient relationships. For hypereutrophic observations, crustacean zooplankton biomass distributions for individual TN intervals overlapped considerably across the entire TN range (Supplemental Fig. S3). Counter to the proposed mechanism, a slight trend toward reduced crustacean zooplankton biomass was observed at the highest TN intervals.

High N sensitivity hypothesis

We evaluated whether high TN concentrations were accompanied by changes in DIN composition that could be interacting with organic carbon pools. For hypereutrophic observations, nitrate composed almost all of TN

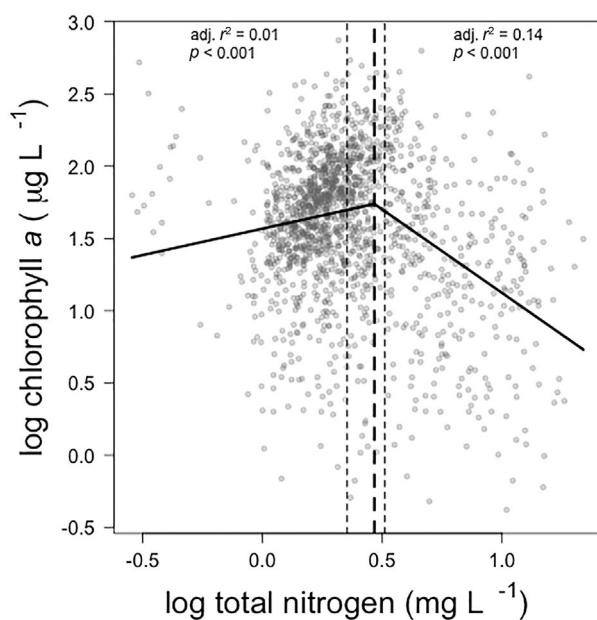


Figure 4. Piecewise linear regression of chlorophyll *a*–total nitrogen relationship restricted to hypereutrophic observations (total phosphorus $> 100 \mu\text{g L}^{-1}$). The thick dashed line represents the estimated change point, whereas the thin dashed lines represent 97.5% confidence intervals of the estimate. Markers representing individual lake observations are transparent, so darker clusters represent overlapping markers. Both variables were \log_{10} -transformed prior to analyses.

for observations in which TN exceeded 3 mg L^{-1} , with ammonia making up a much smaller fraction (Fig. 9), suggesting that nitrate may be playing a prominent role in the underlying mechanism. The maximum nitrate concentration was 19.39 mg L^{-1} (median: 0.17 mg L^{-1}) compared to a maximum ammonium concentration of 1.56 mg L^{-1} (median: 0.03 mg L^{-1}). Additionally, DOC concentrations changed slightly across the TN gradient, where lower DOC distributions co-occurred with the highest TN (Supplemental Fig. S4). Although distributions overlapped considerably below the TN threshold, trends in DOC across TN resembled a unimodal curve, thereby resembling the pattern in Chl-*a* distributions (c.f. Supplemental Fig. S4 and S3c). Despite this similarity, DOC and Chl-*a* were not correlated ($r = 0.06$; $p < 0.050$).

Discussion

In this study, we showed that Chl-*a* covaried with both TN and TP, although relationships between Chl-*a* and TN differed depending on TP concentrations. Although Chl-*a* varied little with increasing TN for mesotrophic or eutrophic observations ($\text{TP} \leq 100 \mu\text{g L}^{-1}$), it displayed a stronger, novel relationship with TN for hypereutrophic observations ($\text{TP} > 100 \mu\text{g L}^{-1}$). Counter to expectations

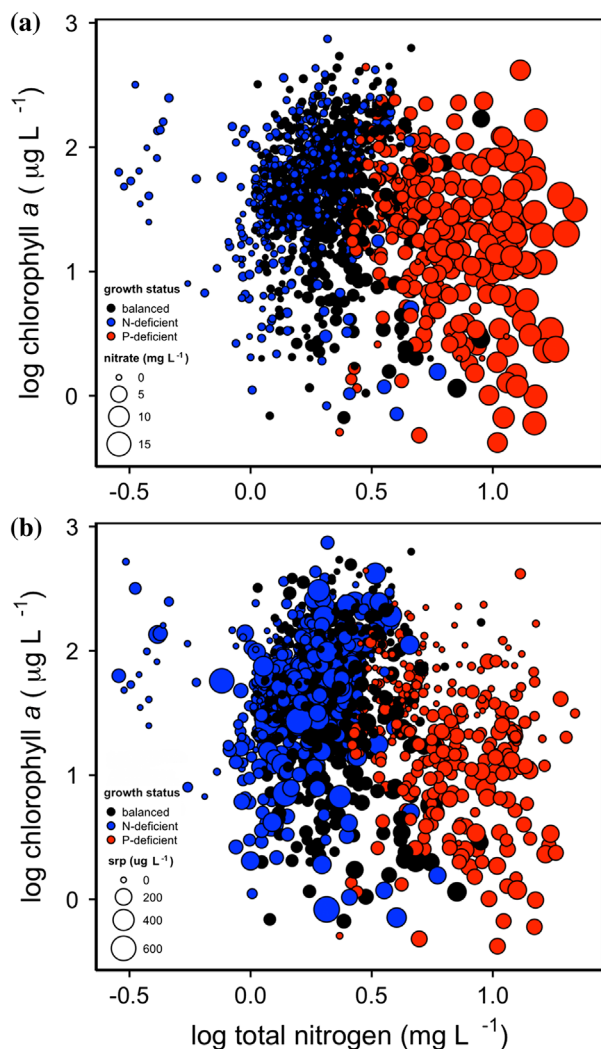


Figure 5. Chlorophyll *a*–total nitrogen relationships for hypereutrophic observations (total phosphorus >100 µg L⁻¹) showing predicted phytoplankton growth deficiency and either (a) nitrate (mg L⁻¹) or (b) soluble reactive phosphorus (µg L⁻¹) concentrations. Chlorophyll *a* and total nitrogen were log₁₀-transformed prior to analyses, whereas dissolved inorganic nutrients were not transformed.

based on nutrient limitation paradigms, Chl-*a* concentrations were greatest under high TP, medium TN conditions but were reduced under the highest nutrient regimes (Fig. 2). As a result, Chl-*a*–TN relationships were best described by a threshold model for hypereutrophic observations in which Chl-*a* was unrelated to TN for TN < 2.93 mg L⁻¹ (97.5% CI: 2.26–3.24 mg L⁻¹) and significantly negatively related to TN beyond this threshold (Fig. 4). The amount of variance in Chl-*a* explained by TN was low for the negative limb, especially compared to the high amounts of variance explained by previous Chl-*a* predictive models (e.g., Dillon and Rigler 1974, Jones and Bachmann 1976, Smith and Shapiro 1981), but was likely influenced by our use of single observational

measurements rather than using seasonal averages as in previous studies (Jones et al. 1998). To our knowledge, this is the first study to document a Chl-*a*–TN threshold relationship in nutrient-enriched lakes. In general, these findings support previous studies demonstrating that TN has little effect on Chl-*a* at low TP but has an increasingly stronger effect in TP-rich lakes (Canfield 1983, McCauley et al. 1989). More important, these findings suggest that nutrient enrichment may produce novel phytoplankton biomass–nutrient relationships in lakes located in intensively human-modified landscapes.

Additionally, trends in Chl-*a* distributions across TN gradients suggested differing Chl-*a*–TN relationships for different trophic conditions. Although TN had little effect on Chl-*a* at low TP, boxplots revealed weak log-sigmoidal relationships between Chl-*a* and TN for mesotrophic and eutrophic observations (Fig. 3a and b). Under these trophic conditions, our findings support previous studies (Prairie et al. 1989, Jones et al. 2008b) demonstrating that relationships between TN and Chl-*a* or the frequency of Chl-*a* > 10 µg L⁻¹ are better approximated as asymptotic relationships (log-log scales). The unimodal relationship for hypereutrophic lakes suggests the form of this relationship is not consistent across all TP ranges, however (Fig. 3c). Numerous studies have documented sigmoidal phytoplankton biomass–TP relationships in lakes, in which Chl-*a* or biomass begins decelerating with increasing TP as other resources become limiting under TP-replete conditions (McCauley et al. 1989, Watson et al. 1992, Filstrup et al. 2014b). Although a similar interpretation could apply to mesotrophic and eutrophic observations in this study, the negative relationship between Chl-*a* and TN beyond the TN threshold suggests a different underlying mechanism was operating under the most nutrient-rich conditions.

Further, regression analyses of all observations demonstrated the importance of both TN and TP as well as underwater light climate ($z_{\text{Secchi}}:z_{\text{mix}}$) in predicting Chl-*a* while also revealing novel interactions among Chl-*a* and TN in this region. In addition to including TP and $z_{\text{Secchi}}:z_{\text{mix}}$, the best Chl-*a* predictive model included linear and squared TN terms and a TN × TP interaction term (Table 2). In contrast to McCauley et al. (1989), TN had significant partial effects on Chl-*a* in this study, whereas TN was only included as a TN × TP interaction term in their study. Although the TN × TP interaction term suggests TN has differing effects on Chl-*a* depending on concurrent TP, the linear and nonlinear TN terms suggest that TN had a stronger overall effect on Chl-*a* for lakes in this region. Similar to our findings, Jones et al. (2008b) found that significant TN terms resulted in a slight improvement in the amount of variance explained by Chl-*a* predictive models compared to TP-only models in a nearby region.

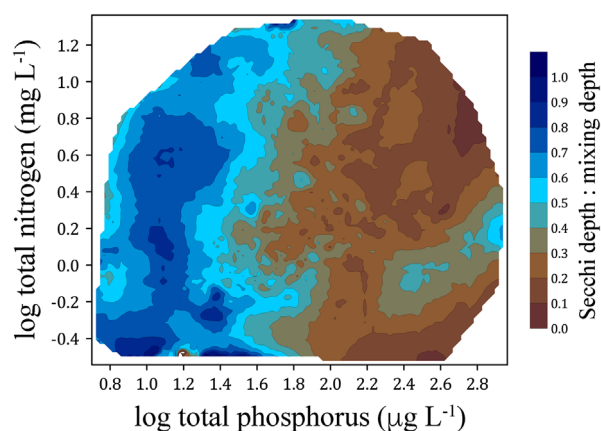


Figure 6. Secchi depth to mixing depth ratio contour plot on total nitrogen vs. total phosphorus nutrient space. Contour lines were generated using second-degree local polynomial regression of lake observational data. Total nitrogen and total phosphorus concentrations were \log_{10} -transformed prior to analyses.

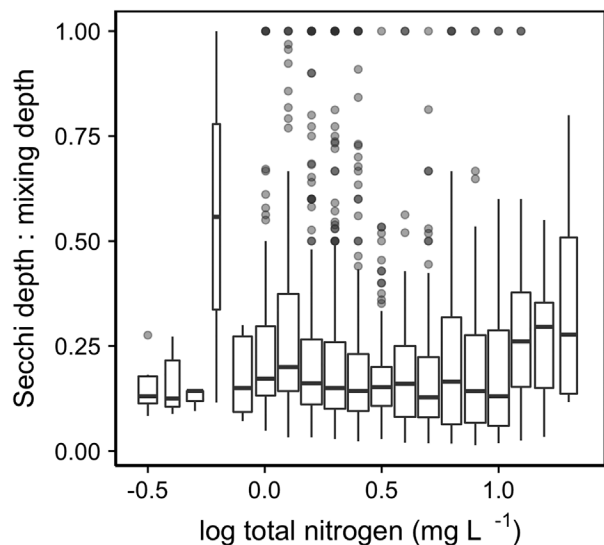


Figure 7. Boxplots of Secchi depth to mixing depth ratios by total nitrogen interval (bin width = 0.1 log total nitrogen) for hypereutrophic (total phosphorus $>100 \mu\text{g L}^{-1}$) observations. Markers representing outliers are transparent, so darker clusters represent overlapping markers. Total nitrogen concentrations were \log_{10} -transformed prior to analyses.

Additionally, the signs of TN terms in our study indicate that the partial effect of TN on Chl-*a* changes from positive to negative with increasing TN, thereby contrasting with previous studies demonstrating positive log-linear partial effects of TN (Smith 1982, Canfield 1983, Jones et al. 2008b). Overall, these findings suggest that either the magnitude of nutrient enrichment in this region, as compared to previous studies, or regional landscape characteristics, which can modify Chl-*a*-nutrient relationships (Jones et al. 2011, Wagner et al. 2011, Filstrup et al. 2014b), are contributing to these novel relationships.

Although correlation does not necessarily imply causation, we were interested in whether any potential underlying mechanisms could have produced the HNLC region observed in this study. First, we tested whether the Chl-*a* threshold response to increasing TN for hypereutrophic observations could be explained by shifting resource limitation across the TN gradient, as demonstrated previously (e.g., McCauley et al. 1989, Prairie et al. 1989). For example, iron deficiency can limit phytoplankton growth in some areas of the ocean, thereby creating high macronutrient (N, P, Si), low Chl-*a* regions (Martin and Fitzwater 1988). Additionally, light availability can limit phytoplankton biomass in lakes, either through phytoplankton self-shading or through large loads of inorganic particles (Jewson 1977, Vörös and Padisák 1991, Jones et al. 2008b). For example, inorganic turbidity can cause reduced Chl-*a* compared to concentrations predicted from nutrients within reservoirs from a nearby region (Jones and Knowlton 2005, Jones et al. 2008b). Variability in growth deficiency status (as inferred from TN:TP; Guildford and Hecky 2000) and underwater light climate ($z_{\text{Secchi}}:z_{\text{mix}}$) across Chl-*a*-TN relationships did not support these mechanisms. TN:TP ratios, combined with commonly low SRP and high nitrate concentrations, suggested consistent P-deficient growth conditions for observations beyond the TN threshold (Fig. 5). Slightly higher $z_{\text{Secchi}}:z_{\text{mix}}$ values for the highest TN intervals indicated that underwater light climate was more favorable within the HNLC region, despite contours indicating relatively low $z_{\text{Secchi}}:z_{\text{mix}}$ (Fig. 6 and 7). Although data on micronutrients are not available, Downing et al. (2016) showed that silica (Si) is not likely limiting production in these Cyanobacteria-dominated systems. Further, Chl-*a* would be unrelated to TN beyond the TN threshold if another factor were limiting, thereby approximating a sigmoidal relationship across the entire TN gradient, as demonstrated for mesotrophic and eutrophic observations in this study (Fig. 3a and b) and in previous Chl-*a*-TP studies (McCauley et al. 1989). The significant negative Chl-*a*-TN relationship beyond the threshold suggests that either high TN negatively affects Chl-*a* or another antagonistic factor coincides with high TN (Fig. 4).

Next, we tested whether seasonal or long-term shifts in phytoplankton community composition could have produced the Chl-*a*-TN threshold relationship as an artifact of fluctuations in cellular Chl-*a* content of dominant taxa. Cellular Chl-*a* content can vary by 2 orders of magnitude (0.1–9.7% of wet weight) across studies and even 5-fold (0.5–23.6 $\mu\text{g mm}^{-3}$ biovolume) within a single lake, depending on phytoplankton composition and environmental conditions (Nicholls and Dillon 1978, Felipe and Catalan 2000). Because Cyanobacteria can have low cellular Chl-*a* content and are predicted to dominate in nutrient-rich lakes (Trimbee and Prepas 1987, Downing

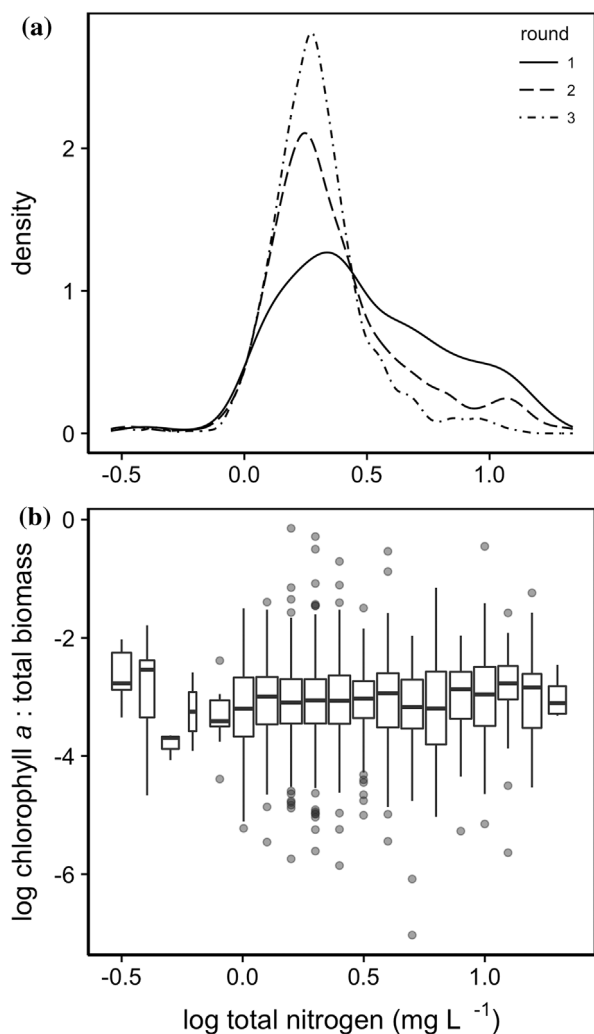


Figure 8. (a) Distribution of observations by sampling round and (b) boxplots of chlorophyll *a* to total phytoplankton biomass ratio across the total nitrogen gradient for hypereutrophic (total phosphorus $>100 \mu\text{g L}^{-1}$) observations. For sampling rounds (a), Round 1 = mid-May–Jun; Round 2 = Jul–mid-Aug; Round 3 = mid-Aug–Sep. For chlorophyll *a*:total biomass (b), total nitrogen bin width = 0.1 log total nitrogen. Markers representing outliers are transparent, so darker clusters represent overlapping markers. Total nitrogen concentrations and chlorophyll *a*:total biomass ratios were \log_{10} -transformed prior to analyses.

et al. 2001, Kasprzak et al. 2008), the HNLC region could have resulted from reduced cellular Chl-*a* content of Cyanobacteria rather than an actual decrease in phytoplankton biomass. Additionally, the amount of Chl-*a* produced per unit TP varies across the trophic gradient as a “hump-shaped” relationship in Missouri reservoirs (Jones et al. 2011), which could also support the finding of low Chl-*a* in nutrient rich waters within the region. Data did not support this mechanism; Chl-*a*:biomass ratios were consistent across the entire TN range of hypereutrophic observations (Fig. 8b), and phytoplankton biomass was also reduced beyond the TN threshold

(Fig. 2b). Additionally, the proportional abundance of Cyanobacteria decreased under high TN (Supplemental Fig. S2), which contradicts this mechanism but supports previous research from this region (Filstrup et al. 2016). Instead, the Chl-*a*–TN threshold relationship seemed to reflect changes in phytoplankton biomass.

Data did support a possible seasonal effect underlying Chl-*a*–TN relationships displayed in this study. High TN concentrations tended to occur more frequently in early summer (Fig. 8a), which may have resulted in high nutrient concentrations occurring before phytoplankton biomass had time to develop under more favorable temperature and light conditions later in the growing season. In this region, N concentrations in receiving streams are typically greater during spring following fertilizer applications and major runoff events, whereas concentrations decrease in summer because of lower runoff and greater in-stream nutrient processing (Becher et al. 2001).

Although the underlying mechanisms likely differ, these seasonal patterns are consistent with those from a nearby region, where observed maximum Chl-*a* commonly exceeded predicted values in late summer, but Chl-*a*:TP ratios were reduced in early summer because of turbid inflows (Jones and Knowlton 2005, Jones et al. 2011). Additionally, Cyanobacteria, which commonly form large blooms within this region (Graham et al. 2004, Filstrup et al. 2016), are favored under warmer temperatures in mid to late summer (Sommer 1986, Reynolds 2006, Paerl and Huisman 2008), which would further contribute to the offset of high Chl-*a* from high TN. The overall decline in Cyanobacteria relative abundance with increasing TN lends support to this mechanism (Supplemental Fig. S2). For this same region, Filstrup et al. (2016) found a similar nonlinear decrease in Cyanobacteria proportional abundance across a TN gradient using data averaged by lake-year, suggesting this relationship may not be simply driven by seasonal phytoplankton phenology.

Next, we tested whether zooplankton grazing pressure could help explain the HNLC region. Zooplankton grazing can strongly affect phytoplankton biomass and composition in lakes (Carpenter et al. 1998), in which zooplankton biomass and body size help explain residual variance in Chl-*a*–TP relationships (Pace 1984, Kamarainen et al. 2008). Most notably, zooplankton grazing pressure can induce a spring clear-water phase common in mesotrophic and eutrophic lakes, although its timing is highly lake dependent (Lampert et al. 1986, Dröscher et al. 2009). Crustacean zooplankton biomass was relatively consistent across the entire TN range of hypereutrophic observations and slightly decreased with increasing TN across the highest TN intervals (Supplemental Fig. S3). Further, this mechanism would suggest that zooplankters were preferentially consuming Cyanobacteria, which are known as

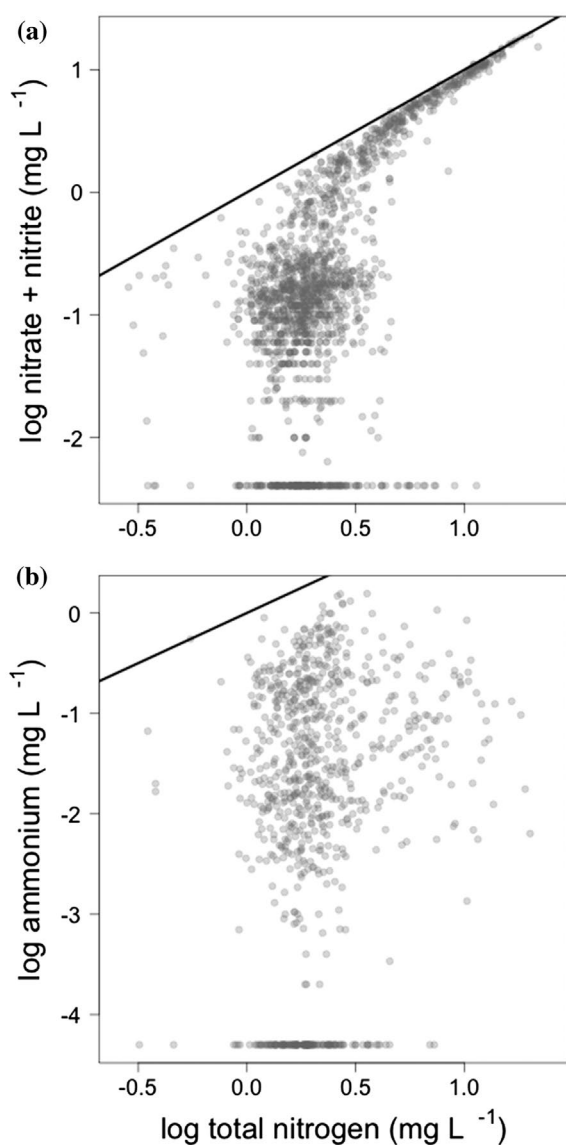


Figure 9. Total nitrogen composition by (a) nitrate + nitrite and (b) ammonium for hypereutrophic (total phosphorus $>100 \mu\text{g L}^{-1}$) observations. Markers representing individual lake observations are transparent, so darker clusters represent overlapping markers. The solid lines represent 1:1 lines for reference. All variables were \log_{10} -transformed prior to analyses.

poor food sources (Wilson et al. 2006, Heathcote et al. 2016), thereby making this an unlikely mechanism.

Finally, we considered whether high TN in these lakes, which was primarily driven by nitrate (Fig. 9a), could have either a direct or indirect negative effect on phytoplankton biomass. For example, nitrate can undergo photolysis under high light irradiance to produce various reactive oxygen species (ROS; e.g., $\cdot\text{NO}_2$, $\cdot\text{OH}$, $^1\text{O}_2$) that can damage organic compounds (Zafiriou 1974, Salin 1988, Vione et al. 2006). In fact, both direct and indirect (ROS-mediated) photolysis of trace organic compounds are well studied as potential contaminant removal

mechanisms in treatment wetlands (Jasper et al. 2013, Jasper and Sedlak 2013). Excited triplet state dissolved organic matter ($^3\text{DOM}^*$) can also produce free radicals by oxidizing water molecules, but nitrate is commonly the primary source of ROS under high nitrate conditions (Takeda et al. 2004, Vione et al. 2006). Although ROS formation through nitrate photolysis has been studied in marine ecosystems since the 1970s (Zafiriou 1974) and are known to indiscriminately oxidize organic matter (Salin 1988), no studies to our knowledge have documented negative impacts of nitrate-derived ROS or other free radicals on phytoplankton in lakes. Concurrent observations of high nitrate and low DOC concentrations beyond the TN threshold may lend support to this mechanism (Fig. 9a; Supplemental Fig. S4). We anticipated similar DOC concentrations across observations because of similar land use and land cover within this region and previous studies demonstrating that lake DOC is largely influenced by terrestrial landscape characteristics (Gergel et al. 1999, Webster et al. 2008). The high occurrence of low DOC observations beyond the TN threshold suggests that some process, potentially negative interactions with nitrate-derived ROS, may have degraded DOC under high nutrient regimes.

Because DOM is a known scavenger for ROS (Brezonik and Fulkerson-Brekken 1998), this hypothesis seems plausible. If observations beyond the TN threshold coincided with low DOC inflows, however, then ROS may have been more damaging to phytoplankters because of reduced scavenging by DOC. Although chloroplasts have evolved defence mechanisms to protect against damage from ROS (Salin 1988), accumulation of ROS in the water column through nitrate photolysis may be placing added strain on these mechanisms. Alternatively, these findings may indicate that large storm pulses are delivering large nutrient loads low in DOC to lakes (Dalzell et al. 2011), which may promote high rates of ROS formation after storms pass.

A plausible ROS mechanism requires an underwater light climate (especially with respect to ultraviolet [UV] wavelengths) conducive to promoting nitrate photolysis, despite a euphotic zone restricted to the surface layer in these highly productive lakes. In fact, algal self-shading has been demonstrated to reduce oxidative stress in experimental mesocosms, although whether this phenomenon occurs in natural environments is unclear (Barros et al. 2003). Agricultural practices can modify underwater light climate by increasing both abiotic and biogenic turbidity through increased sediment and nutrient loading, respectively (Allan et al. 1997, North et al. 2013). The predominance of surface bloom-forming Cyanobacteria in these lakes also contributes to reduced light penetration (Filstrup et al. 2016). By contrast, Zepp et al. (1987) showed that hydroxyl radical ($\cdot\text{OH}$) production rates in

Greifensee were comparable to the open ocean because much higher nitrate concentrations compensated for reduced solar irradiance and light penetration, suggesting that nitrate photolysis can be an important source of ROS in nitrate-rich, productive lakes. Although delayed initiation of nitrate photolysis in these systems may be due to UV light attenuation, $\cdot\text{OH}$ production rates are commonly much more rapid than lake flushing rates, which can result in accumulation of ROS in the water column (Zepp et al. 1987).

If accumulation of ROS through nitrate photolysis was the primary mechanism causing the HNLC region, then the low TN threshold observed in this study (2.93 mg L^{-1}) leads to the speculation that Chl-*a*-TN threshold relationships should be common in nutrient-rich lakes from other agricultural regions worldwide. Yet, to our knowledge, this relationship has not been previously demonstrated by empirical studies using existing monitoring datasets. For example, Chl-*a*-nutrient relationships have been studied extensively in reservoirs in Missouri, which shares Iowa's southern border, using long-term monitoring data without producing similar results (e.g., Jones et al. 2008b, 2011). Despite the proximity of these 2 regions, landscape characteristics may contribute to different biogeochemical nutrient cycles within their watersheds. In a cross-regional comparison, Jones et al. (2008a) demonstrated that reservoirs in southern Iowa had ~2-fold higher nutrient concentrations than reservoirs in the Missouri Plains. Further, Missouri reservoirs tend to have lower TN relative to TP compared to empirical models based on world lakes (Jones et al. 2008b). Whereas TN and TP (\log_{10} -transformed) were weakly correlated in Iowa lakes ($r^2 = 0.10$), they were tightly coupled in Missouri reservoirs ($r^2 = 0.84$), resulting in Chl-*a*-TN relationships strongly approximating Chl-*a*-TP relationships (Jones et al. 2008b). The Missouri dataset therefore contains more densely populated data at the lower nutrient end of the relationship, suggesting that agricultural practices and landscape characteristics were not driving the extreme nutrient concentrations needed to reveal the Chl-*a* threshold response to TN. Note that relationships from Missouri were illustrated using lake-wide average data instead of individual sampling event data, as in this study.

Additionally, several other characteristics can influence phytoplankton-nutrient relationships in lakes, which may help explain why previous studies have not documented similar threshold responses. For this mechanism to hold, high TN concentrations must be driven by nitrate rather than other forms of dissolved inorganic or organic N (DIN and DON, respectively) and therefore would not be observed in regions where agricultural N amendments are not oxidized to nitrate through soil microbial processes before entering receiving waters. Note

that these monitoring data were collected at the historically maximum depth location in each lake, whereas nitrate concentrations commonly exceed 30 mg L^{-1} in inflowing streams (Filstrup and Downing unpubl.). In addition to region-specific agricultural practices, other regional factors (e.g., climate, hydrology, geology) may influence production and accumulation of ROS in the water column. For example, Jones et al. (2008a) found flushing rates accounted for almost twice the variability in TP for Missouri reservoirs compared to those in southern Iowa, suggesting that flushing rates may have a stronger influence on phytoplankton-nutrient relationships in Missouri. Bicarbonate and carbonate ions are known scavengers of free radicals in well-buffered systems (Brezonik and Fulkerson-Brekken 1998), so ROS may not accumulate in lakes within limestone regions.

Finally, the level of data aggregation prior to analyses may have influenced the form of Chl-*a*-TN relationships demonstrated here compared to previous studies. Although we used individual sampling observations to consider the widest range in nutrients, previous studies typically aggregated data by seasonal or lake-wide averages (e.g., Dillon and Rigler 1974, Jones and Bachmann 1976, Smith and Shapiro 1981). Aggregating data by averages could have influenced phytoplankton-nutrient relationships by (1) reducing nutrient ranges by "averaging out" the extreme nutrient concentrations needed to reveal threshold responses and (2) reducing variability in response and predictor variables that helped contribute to extremely high levels of Chl-*a* variance explained by previous predictive models (commonly $r^2 > 0.90$).

In this study, numerous observations had TN concentrations $>10 \text{ mg L}^{-1}$ (Fig. 4). Compared to modeling log-linear relationships, threshold relationships on \log_{10} -transformed scales require increasingly more observations to accurately estimate the breakpoint and to maintain adequate statistical power to model both limbs. By analyzing the same dataset using different levels of data aggregation, Jones et al. (1998) showed that the amount of \log_{10} Chl-*a* variance explained by TP increased from 52% for individual sampling observations to 84% for lake-wide averages, and the form of the model seemed more nonlinear for the unaggregated data. Further investigation of Chl-*a*, TN, and TP relationships from other hypereutrophic waters using different levels of data aggregation is warranted to determine whether negative effects of nitrate-derived ROS on Chl-*a* are common elsewhere.

Conclusions

Although mechanisms underlying these relationships require further study, our findings suggest that agricultural practices, including large nutrient amendments to

croplands, may produce novel ecological contexts that alter phytoplankton biomass–nutrient relationships in lakes. In this region, management strategies aimed at reducing both N and P to curb cultural eutrophication may result in increases in Chl-*a* in lakes where both nitrate ($\geq 3 \text{ mg L}^{-1}$) and TP ($>100 \text{ } \mu\text{g L}^{-1}$) are high, but N reductions may not be effective at reducing Chl-*a* in lakes where TP is $\leq 100 \text{ } \mu\text{g L}^{-1}$. As a result, increased nitrate concentrations may fuel the illusion of improved water quality because of decreased Chl-*a* in hypereutrophic lakes. Further, extreme N concentrations may lead to temporal trends that do not show increased Chl-*a* or reduced water transparency, even as nutrient concentrations reach high levels.

Our findings do not support a P-only management paradigm but simply suggest that water quality may worsen until a TN threshold is crossed. Further, recent studies demonstrating reduced N removal through denitrification and nitrate accumulation in some lakes due to P loading reductions (Finlay et al. 2013) indicate that nitrate-derived ROS formation may be stimulated under P-only management strategies in this region, which may have unanticipated effects on pelagic community structure and function. Because demand for agricultural products will likely increase in the future, our study region likely serves as a temporal analogue for other areas of extreme nutrients; therefore, Chl-*a*–TN threshold relationships may be more common under future high nutrient regimes.

Acknowledgements

Funding for this research was provided by the Iowa Department of Natural Resources (Award # 2014ESDGSBMBalm0004) to JAD and CTF and by the National Science Foundation (DEB-1021525; EF-1065649) to JAD. We thank Iowa State University Limnology Laboratory professional scientists Amber Erickson, Dan Kendall, and Lisa Whitehouse who supervised the collection and analyses of all samples. We thank the numerous undergraduate field and laboratory technicians from Iowa State University, who have collected water samples and performed water quality analyses for this project. We also thank Yves T. Prairie and Peter R. Leavitt for suggesting alternate mechanisms that could be underlying the HNLC region.

Funding

This work was supported by the National Science Foundation [DEB-1021525; EF-1065649] and the Iowa Department of Natural Resources [2014ESDGSBMBalm004].

ORCID

Christopher T. Filstrup  <http://orcid.org/0000-0003-3812-2831>

John A. Downing  <http://orcid.org/0000-0001-8547-0789>

References

- Allan JD, Erickson DL, Fay J. 1997. The influence of catchment land use on stream integrity across multiple spatial scales. *Freshwater Biol.* 37:149–161.
- Allgeier JE, Rosemond AD, Layman CA. 2011. The frequency and magnitude of non-additive responses to multiple nutrient enrichment. *J Appl Ecol.* 48:96–101.
- [APHA] American Public Health Association. 1998. Standard methods for the examination of water and wastewater. 20th ed. Washington (DC): American Public Health Association; American Water Works Association; Water Environment Federation.
- Arar EJ, Collins GB. 1997. US Environmental Protection Agency method 445.0: in vitro determination of chlorophyll *a* and pheophytin *a* in marine and freshwater algae by fluorescence. Cincinnati (OH): US Environmental Protection Agency.
- Arbuckle KE, Downing JA. 2001. The influence of watershed land use on lake N: P in a predominantly agricultural landscape. *Limnol Oceanogr.* 46:970–975.
- Barros MP, Pedersén M, Colepicolo P, Snoeijs P. 2003. Self-shading protects phytoplankton communities against H_2O_2 -induced oxidative damage. *Aquat Microb Ecol.* 30:275–282.
- Becher KD, Kalkhoff SJ, Schnoebelen DJ, Barnes KK, Miller VE. 2001. Water-quality assessment of the Eastern Iowa Basins-nitrogen, phosphorus, suspended sediment, and organic carbon in surface water, 1996–98. Iowa City (IA): US Geological Survey. Report No. 01-4175.
- Bracken MES, Hillebrand H, Borer ET, Seabloom EW, Cebrian J, Cleland EE, Elser JJ, Gruner DS, Harpole WS, Ngai JT, Smith JE. 2015. Signatures of nutrient limitation and co-limitation: responses of autotroph internal nutrient concentrations to nitrogen and phosphorus additions. *Oikos.* 124:113–121.
- Brezonik PL, Fulkerson-Brekken J. 1998. Nitrate-induced photolysis in natural waters: controls on concentrations of hydroxyl radical photo-intermediates by natural scavenging agents. *Environ Sci Technol.* 32:3004–3010.
- Canfield DE Jr. 1983. Prediction of chlorophyll *a* concentrations in Florida lakes: the importance of phosphorus and nitrogen. *J Am Water Resour Assoc.* 19:255–262.
- Carpenter SR, Cole JJ, Mitchell JF, Pace ML. 1998. Impact of dissolved organic carbon, phosphorus, and grazing on phytoplankton biomass and production in experimental lakes. *Limnol Oceanogr.* 43:73–80.
- Crompton WG, Isenhardt TM, Mitchell PD. 1992. Nitrate and organic N analyses with second-derivative spectroscopy. *Limnol Oceanogr.* 37:907–913.
- Dalzell BJ, King JY, Mulla DJ, Finlay JC, Sands GR. 2011. Influence of subsurface drainage on quantity and quality of dissolved organic matter export from agricultural landscapes. *J Geophys Res.* 116:1–13.
- Dillon PJ, Rigler FH. 1974. The phosphorus-chlorophyll relationship in lakes. *Limnol Oceanogr.* 19:767–773.
- Downing JA, Cherrier CT, Fulweiler RW. 2016. Low ratios of silica to dissolved nitrogen supplied to rivers arise from agriculture not reservoirs. *Ecol Lett.* 19:1414–1418.
- Downing JA, McCauley E. 1992. The nitrogen:phosphorus relationship in lakes. *Limnol Oceanogr.* 37:936–945.
- Downing JA, Watson SB, McCauley E. 2001. Predicting Cyanobacteria dominance in lakes. *Can J Fish Aquat Sci.* 58:1905–1908.

- Dröscher I, Patoine A, Finlay K, Leavitt PR. 2009. Climate control of the spring clear-water phase through the transfer of energy and mass to lakes. *Limnol Oceanogr.* 54:2469–2480.
- Dumont HJ, Van de Velde I, Dumont S. 1975. The dry weight estimate of biomass in a selection of Cladocera, Copepoda and Rotifera from the plankton, periphyton and benthos of continental waters. *Oecologia.* 19:75–97.
- Edmondson WT. 1970. Phosphorus, nitrogen, and algae in Lake Washington after diversion of sewage. *Science.* 169:690–691.
- Elser JJ, Bracken MES, Cleland EE, Gruner DS, Harpole WS, Hillebrand H, Ngai JT, Seabloom EW, Shurin JB, Smith JE. 2007. Global analysis of nitrogen and phosphorus limitation of primary producers in freshwater, marine and terrestrial ecosystems. *Ecol Lett.* 10:1135–1142.
- Felip M, Catalan J. 2000. The relationship between phytoplankton biovolume and chlorophyll in a deep oligotrophic lake: decoupling in their spatial and temporal maxima. *J Plankton Res.* 22:91–105.
- Filstrup CT, Heathcote AJ, Kendall DL, Downing JA. 2016. Phytoplankton taxonomic compositional shifts across nutrient and light gradients in temperate lakes. *Inland Waters.* 6:234–249.
- Filstrup CT, Hillebrand H, Heathcote AJ, Harpole WS, Downing JA. 2014a. Cyanobacteria dominance influences resource use efficiency and community turnover in phytoplankton and zooplankton communities. *Ecol Lett.* 17:464–474.
- Filstrup CT, Wagner T, Soranno PA, Stanley EH, Stow CA, Webster KE, Downing JA. 2014b. Regional variability among nonlinear chlorophyll–phosphorus relationships in lakes. *Limnol Oceanogr.* 59:1691–1703.
- Finlay JC, Small GE, Sterner RW. 2013. Human influences on nitrogen removal in lakes. *Science.* 342:247–250.
- Fraterrigo JM, Downing JA. 2008. The influence of land use on lake nutrients varies with watershed transport capacity. *Ecosystems.* 11:1021–1034.
- Gergel SE, Turner MG, Kratz TK. 1999. Dissolved organic carbon as an indicator of the scale of watershed influence on lakes and rivers. *Ecol Appl.* 9:1377–1390.
- Gibson CA, O'Reilly CM, Conine AL, Lipshutz SM. 2015. Nutrient uptake dynamics across a gradient of nutrient concentrations and ratios at the landscape scale. *J Geophys Res Biogeosci.* 120:326–340.
- Graham JL, Jones JR, Jones SB, Downing JA, Clevenger TE. 2004. Environmental factors influencing microcystin distribution and concentration in the Midwestern United States. *Water Res.* 38:4395–4404.
- Guildford SJ, Hecky RE. 2000. Total nitrogen, total phosphorus, and nutrient limitation in lakes and oceans: is there a common relationship? *Limnol Oceanogr.* 45:1213–1223.
- Haney JF, Hall DJ. 1973. Sugar-coated *Daphnia*: a preservation technique for Cladocera. *Limnol Oceanogr.* 18:331–333.
- Hayes NM, Vanni MJ, Horgan MJ, Renwick WH. 2015. Climate and land use interactively affect lake phytoplankton nutrient limitation status. *Ecology.* 96:392–402.
- Heathcote AJ, Downing JA. 2012. Impacts of eutrophication on carbon burial in freshwater lakes in an intensively agricultural landscape. *Ecosystems.* 15:60–70.
- Heathcote AJ, Filstrup CT, Kendall D, Downing JA. 2016. Biomass pyramids in lake plankton: influence of Cyanobacteria size and abundance. *Inland Waters.* 6:250–257.
- Hillebrand H, Dürselen C-D, Kirschtel D, Pollinger U, Zohary T. 1999. Biovolume calculation for pelagic and benthic microalgae. *J Phycol.* 35:403–424.
- Howarth RW, Billen G, Swaney D, Townsend A, Jaworski N, Lajtha K, Downing JA, Elmgren R, Caraco N, Jordan T, et al. 1996. Regional nitrogen budgets and riverine N & P fluxes for the drainages to the North Atlantic Ocean: natural and human influences. *Biogeochemistry.* 35:75–139.
- Jasper JT, Nguyen MT, Jones ZL, Ismail NS, Sedlak DL, Sharp JO, Luthy RG, Horne AJ, Nelson KL. 2013. Unit process wetlands for removal of trace organic contaminants and pathogens from municipal wastewater effluents. *Environ Eng Sci.* 30:421–436.
- Jasper JT, Sedlak DL. 2013. Phototransformation of wastewater-derived trace organic contaminants in open-water unit process treatment wetlands. *Environ Sci Technol.* 47:10781–10790.
- Jewson DH. 1977. Light penetration in relation to phytoplankton content of the euphotic zone of Lough Neagh. N. Ireland. *Oikos.* 28:74–83.
- Jones JR, Bachmann RW. 1976. Prediction of phosphorus and chlorophyll levels in lakes. *J Water Pollut Control Fed.* 48:2176–2182.
- Jones JR, Borofka BP, Bachmann RW. 1976. Factors affecting nutrient loads in some Iowa streams. *Water Res.* 10:117–122.
- Jones JR, Knowlton MF, Swar DB. 1989. Limnological reconnaissance of waterbodies in central and southern Nepal. *Hydrobiologia.* 184:171–189.
- Jones JR, Knowlton MF, Kaiser MS. 1998. Effects of aggregation on chlorophyll-phosphorus relations in Missouri reservoirs. *Lake Reserv Manage.* 14:1–9.
- Jones JR, Knowlton MF. 2005. Chlorophyll response to nutrients and non-algal seston in Missouri reservoirs and oxbow lakes. *Lake Reserv Manage.* 21:361–371.
- Jones JR, Knowlton MF, Obrecht DV. 2008a. Role of land cover and hydrology in determining nutrients in mid-continent reservoirs: implications for nutrient criteria and management. *Lake Reserv Manage.* 24:1–9.
- Jones JR, Obrecht DV, Perkins BD, Knowlton MF, Thorpe AP, Watanabe S, Bacon RR. 2008b. Nutrients, seston, and transparency of Missouri reservoirs and oxbow lakes: an analysis of regional limnology. *Lake Reserv Manage.* 24:155–180.
- Jones JR, Obrecht DV, Thorpe AP. 2011. Chlorophyll maxima and chlorophyll: total phosphorus ratios in Missouri reservoirs. *Lake Reserv Manage.* 27:321–328.
- Kalff J. 2001. *Limnology*. 2nd ed. Upper Saddle River (NJ): Prentice Hall.
- Kamarainen AM, Rowland FE, Biggs R, Carpenter SR. 2008. Zooplankton and the total phosphorus – chlorophyll a relationship: hierarchical Bayesian analysis of measurement error. *Can J Fish Aquat Sci.* 65:2644–2655.
- Kasprzak P, Padisák J, Koschel R, Krienitz L, Gervais F. 2008. Chlorophyll *a* concentration across a trophic gradient of lakes: an estimator of phytoplankton biomass? *Limnologia.* 38:327–338.
- Lampert W, Fleckner W, Rai H, Taylor BE. 1986. Phytoplankton control by grazing zooplankton: a study on the spring clear-water phase. *Limnol Oceanogr.* 31:478–490.
- Lund JWG, Kipling C, Le Cren ED. 1958. The inverted microscope method of estimating algal numbers and the

- statistical basis of estimations by counting. *Hydrobiologia*. 11:143–170.
- Martin JH, Fitzwater SE. 1988. Iron deficiency limits phytoplankton growth in the north-east Pacific subarctic. *Nature*. 331:341–343.
- McCauley E. 1984. The estimation of the abundance and biomass of zooplankton in samples. In: Downing JA, Rigler FH, editors. *A manual on methods for the assessment of secondary production in fresh waters*. Oxford: Blackwell Scientific Publications; p. 228–265.
- McCauley E, Downing JA, Watson S. 1989. Sigmoid relationships between nutrients and chlorophyll among lakes. *Can J Fish Aquat Sci*. 46:1171–1175.
- Nicholls KH, Dillon PJ. 1978. An evaluation of phosphorus-chlorophyll-phytoplankton relationships for lakes. *Int Rev Hydrobiol*. 63:141–154.
- North RL, Winter JG, Dillon PJ. 2013. Nutrient indicators of agricultural impacts in the tributaries of a large lake. *Inland Waters*. 3:221–234.
- Pace ML. 1984. Zooplankton community structure, but not biomass, influences the phosphorus–chlorophyll a relationship. *Can J Fish Aquat Sci*. 41:1089–1096.
- Paerl HW, Huisman J. 2008. Blooms like it hot. *Science*. 320:57–58.
- Paerl HW, Scott JT, McCarthy MJ, Newell SE, Gardner W, Havens KE, Hoffman DK, Wilhelm SW, Wurtsbaugh WA. 2016. It takes two to tango: when and where dual nutrient (N & P) reductions are needed to protect lakes and downstream ecosystems. *Environ Sci Technol*. 50:10805–10813.
- Prairie YT, Duarte CM, Kalff J. 1989. Unifying nutrient–chlorophyll relationships in lakes. *Can J Fish Aquat Sci*. 46:1176–1182.
- R Core Team. 2016. R: a language and environment for statistical computing.
- Reynolds CS. 2006. *The ecology of phytoplankton*. Cambridge (UK): Cambridge University Press.
- Sakamoto M. 1966. Primary production by phytoplankton community in some Japanese lakes and its dependence on lake depth. *Arch Hydrobiol*. 62:1–28.
- Salin ML. 1988. Toxic oxygen species and protective systems of the chloroplast. *Physiol Plant*. 72:681–689.
- Schindler DW. 1977. Evolution of phosphorus limitation in lakes. *Science*. 195:260–262.
- Schindler DW, Carpenter SR, Chapra SC, Hecky RE, Orihel DM. 2016. Reducing phosphorus to curb lake eutrophication is a success. *Environ Sci Technol*. 50:8923–8929.
- Schindler DW, Hecky RE, Findlay DL, Stainton MP, Parker BR, Paterson MJ, Beaty KG, Lyng M, Kasian SEM. 2008. Eutrophication of lakes cannot be controlled by reducing nitrogen input: results of a 37-year whole-ecosystem experiment. *Proc Nat Acad Sci*. 105:11254–11258.
- Scott JT, McCarthy MJ. 2010. Nitrogen fixation may not balance the nitrogen pool in lakes over timescales relevant to eutrophication management. *Limnol Oceanogr*. 55:1265–1270.
- Smith VH. 1982. The nitrogen and phosphorus dependence of algal biomass in lakes: an empirical and theoretical analysis. *Limnol Oceanogr*. 27:1101–1112.
- Smith VH, Shapiro J. 1981. Chlorophyll-phosphorus relations in individual lakes: their importance to lake restoration strategies. *Environ Sci Technol*. 15:444–451.
- Sommer U. 1986. The periodicity of phytoplankton in Lake Constance (Bodensee) in comparison to other deep lakes of central Europe. *Hydrobiologia*. 138:1–7.
- Sonderegger DL. 2012. SiZer: significant zero crossings. Version 0.1-4. <https://CRAN.R-project.org/package=SiZer>
- Stanley EH, Maxted JT. 2008. Changes in the dissolved nitrogen pool across land cover gradients in Wisconsin streams. *Ecol Appl*. 18:1579–1590.
- Stenback GA, Crumpton WG, Schilling KE, Helmers MJ. 2011. Rating curve estimation of nutrient loads in Iowa rivers. *J Hydrol*. 396:158–169.
- Sterner RW. 2008. On the phosphorus limitation paradigm for lakes. *Int Rev Hydrobiol*. 93:433–445.
- Takeda K, Takedoi H, Yamaji S, Ohta K, Sakugawa H. 2004. Determination of hydroxyl radical photoproduction rates in natural waters. *Anal Sci*. 20:153–158.
- Trimbee AM, Prepas EE. 1987. Evaluation of total phosphorus as a predictor of the relative biomass of blue-green algae with emphasis on Alberta lakes. *Can J Fish Aquat Sci*. 44:1337–1342.
- [USEPA] US Environmental Protection Agency. 1993. US Environmental Protection Agency Method 350.1, Determination of ammonia nitrogen by semi-automated colorimetry. O'Dell JW, editor. Cincinnati (OH): US Environmental Protection Agency.
- Vanni MJ, Renwick WH, Bowling AM, Horgan MJ, Christian AD. 2011. Nutrient stoichiometry of linked catchment-lake systems along a gradient of land use. *Freshwater Biol*. 56:791–811.
- Vione D, Falletti G, Maurino V, Minero C, Pelizzetti E, Malandrino M, Ajassa R, Olariu R-I, Arsene C. 2006. Sources and sinks of hydroxyl radicals upon irradiation of natural water samples. *Environ Sci Technol*. 40:3775–3781.
- Vollenweider RA. 1968. *Scientific fundamentals of the eutrophication of lakes and flowing waters, with particular reference to nitrogen and phosphorus as factors in eutrophication*. Paris (France): Organisation for Economic Co-operation and Development.
- Vörös L, Padisák J. 1991. Phytoplankton biomass and chlorophyll-a in some shallow lakes in central Europe. *Hydrobiologia*. 215:111–119.
- Wagner T, Soranno PA, Webster KE, Cheruvilil KS. 2011. Landscape drivers of regional variation in the relationship between total phosphorus and chlorophyll in lakes. *Freshwater Biol*. 56:1811–1824.
- Watson S, McCauley E, Downing JA. 1992. Sigmoid relationships between phosphorus, algal biomass, and algal community structure. *Can J Fish Aquat Sci*. 49:2605–2610.
- Webster KE, Soranno PA, Cheruvilil KS, Bremigan MT, Downing JA, Vaux PD, Asplund TR, Bacon LC, Connor J. 2008. An empirical evaluation of the nutrient-color paradigm for lakes. *Limnol Oceanogr*. 53:1137–1148.
- Wickham H. 2009. *ggplot2: elegant graphics for data analysis*. New York (NY): Springer-Verlag.
- Wilson AE, Sarnelle O, Tillmanns AR. 2006. Effects of cyanobacterial toxicity and morphology on the population growth of freshwater zooplankton: meta-analyses of laboratory experiments. *Limnol Oceanogr*. 51:1915–1924.

- Wright SW, Jeffrey SW, Mantoura RFC. 1997. Evaluation of methods and solvents for pigment extraction. In: Jeffrey SW, Mantoura RFC, Wright SW, editors. *Phytoplankton pigments in oceanography: guidelines to modern methods*. Paris (France): UNESCO; p. 261–282.
- Yuan LL, Pollard AI. 2014. Classifying lakes to improve precision of nutrient–chlorophyll relationships. *Freshwater Sci.* 33:1184–1194.
- Zafriou OC. 1974. Sources and reactions of OH and daughter radicals in seawater. *J Geophys Res.* 79:4491–4497.
- Zepp RG, Holgne J, Bader H. 1987. Nitrate-induced photooxidation of trace organic chemicals in water. *Environ Sci Technol.* 21:443–450.